Pharm Res (2015) 32:1957–1974
DOI 10.1007/s11095-014-1589-7

RESEARCH PAPER

New Techniques to Assess *In Vitro* Release of siRNA from Nanoscale Polyplexes

Bettina Krieg • Markus Hirsch • Erik Scholz • Lutz Nuhn • Ilja Tabujew • Heiko Bauer • Sandra Decker • Andriy Khobta • Manfred Schmidt • Wolfgang Tremel • Rudolf Zentel • Kalina Peneva • Kaloian Koynov • A. James Mason • Mark Helm

Received: 21 August 2014 / Accepted: 24 November 2014 / Published online: 9 December 2014

ABSTRACT

Purpose Release of siRNA from nanoscale polyplexes is a crucial yet little investigated process, important during all stages of therapeutic research. Here we develop new methods to characterize polyplex stability early on in the development of new materials.

Methods We used double fluorescent labeled siRNA to compare binding and stability of a panel of chemically highly diverse nanoscale polyplexes, including peptides, lipids, nanohydrogels, poly-L-lysine brushes, HPMA block copolymers and manganese oxide particles. Conventional EMSA and heparin competition methods were contrasted with a newly developed microscale thermophoresis (MST) assay, a near-equilibrium method that allows free choice of buffer conditions. Integrity of FRET-labeled siRNA was monitored in the presence of nucleases, in cell culture medium and inside living cells. This approach characterizes all relevant steps from polyplex stability, over uptake to *in vitro* knockdown capability.

Results Diverging polyplex binding properties revealed drawbacks of conventional EMSA and heparin competition assays, where MST and FRET-based siRNA integrity measurements offered a better discrimination of differential binding strength. Since cell culture medium left siRNA in all polyplexes essentially intact, the relevant degradation events could be pinpointed to occur inside cells. Differential binding strength of the variegated polyplexes correlated only partially with intracellular degradation. The most successful compounds in RNAi showed intermediate binding strength in our assays.

Conclusions We introduce new methods for the efficient and informative characterization of siRNA polyplexes with special attention to stability. Comparing FRET-labeled siRNA in different polyplexes associates successful knockdown with intermediate siRNA stability in various steps from formulation to intracellular persistence.

KEY WORDS FRET · nuclease resistance · release · siRNA · thermophoresis

ABBREVIATIONS

BR_{50}	50% binding ratio
cc_1	Lowest m/m ratio at which complexation exceeds 95%
CLSM	Confocal laser scanning microscopy
CPP	Cell penetrating peptide
DAB	Diaminobutane-dendrimer-$(NH_2)_{64}$
DOTAP	1,2-dioleoyl-3-trimethylammonium-propane
EMSA	Electrophoretic mobility shift assay
FACS	Fluorescence activated cell sorting

Bettina Krieg and Markus Hirsch have an equal contribution to this paper.

Electronic supplementary material The online version of this article (doi:10.1007/s11095-014-1589-7) contains supplementary material, which is available to authorized users.

B. Krieg • M. Hirsch • E. Scholz • A. Khobta • M. Helm (✉)
Institute of Pharmacy and Biochemistry, Johannes Gutenberg-University Mainz, Staudinger Weg 5, 55128 Mainz, Germany
e-mail: mhelm@uni-mainz.de

L. Nuhn • H. Bauer • S. Decker • M. Schmidt • W. Tremel • R. Zentel
Department of Chemistry, Johannes Gutenberg-University Mainz, Mainz Germany

I. Tabujew • K. Peneva • K. Koynov
Max Planck Institute for Polymer Research, Mainz, Germany

A. J. Mason
Institute of Pharmaceutical Science, King's College London, London, UK

FCS	Fluorescence correlation spectroscopy
FRET	Förster resonance energy transfer
HPMA	N-(2-hydroxypropyl) methacrylamide
m/m	$Mass^{Particle}/mass^{siRNA}$ ratio
$MnO@SiO_2$ particle	Manganese oxide particle covered with silica
MST	Microscale thermophoresis
PAMAM	Poly(amido amine)
pDMAEMA	Poly(2-dimethylamino)ethyl methacrylate
PEI	Polyethyleneimine
PLL	Poly-L-lysine
PVA	Polyvinylalcohol
R/G	Red/green, ratio of acceptor emission to donor emission
R_h	Hydrodynamic radius
z^-_{Hep}/z^-_{RNA}	Negative charges of heparin per negative charges of siRNA

INTRODUCTION

Delivery of siRNA into cells has grown into an important issue in the RNAi field, for therapeutic as well as for fundamental research. The use of nanoscale delivery systems has developed into a research area of its own right, mainly owing to two facts. First, unformulated, *i.e.* "naked" siRNA is fast degraded by nucleases present in blood and cell culture medium, even when the RNA is extensively equipped with stabilizing chemical modifications. Second, naked siRNA, due to its ionic nature, does not readily pass biological membranes. Although a few cell types can take up naked RNA (1), transfection into the vast majority of cell types requires vehicles, typically nanoscale particles that may carry the siRNA as a payload according to a variety of formulation principles. Applications of siRNA in cell culture are extremely wide spread as a tool in fundamental research, but therapeutic applications are subject to intensive exploration as well. For applications *in vivo*, several extra layers of complications enter the search for suitable delivery systems, *i.e.* renal excretion, unspecific uptake, or binding to serum proteins. Furthermore, requirements change after penetration into the cytosol of the target cell. While binding of siRNA to the carrier needs to be tight enough to prevent dissociation outside the cell, siRNA must be released from its carrier once it has entered the cytosol, *e.g.* after escape from endosomes. siRNA must then be incorporated into RNA induced silencing complexes (RISC), the actual effective entities in RNAi. Clearly, the kinetics of release must be major determinants of the availability of siRNA for RISC formation, and, thus, efficiency and duration of the RNAi effect itself. However, successful transfection agents, whose release properties are favorable by definition, have been found empirically, rather than through an understanding of physicochemically determined release properties. One would therefore anticipate significant further progress in the development, if such studies could be based on experimental evaluation of release properties. Meaningful and fast *in vitro* characterization of release parameters would foster the design of new compounds, based on rational analysis rather than on serendipity.

Compounds Investigated for Polyplex Formation

Polyplexes are complexes of nucleic acids such as siRNA, plasmid DNA or oligodeoxynucleotides (ODN) with cationic compounds that rely mainly on ionic interaction. They form nanosized aggregates, which have been used in transfection experiments with great success (2–4). Indeed, the commercial gold standard transfection agents are cationic lipids that form a sub-category of polyplexes termed lipoplexes. The plethora of cationic compounds used to form polyplexes includes 1,2-dioleoyl-3-trimethylammonium-propane (DOTAP) (5), poly(amido amine)s (PAMAM) (4), polyvinylalcohols (PVA) (6), poly-L-lysine (PLL) (7), polycationic cell penetrating peptides (CPP) (8,9), polyethyleneimine (PEI) (10), poly(2-dimethylamino)ethyl methacrylate (pDMAEMA) (11), diaminobutane-dendrimer-$(NH_2)_{64}$ (DAB) (11), and various other compounds(2,3,12).

Indeed, while some inroads have been made to correlate binding properties with knockdown efficiency (13,14), it is still largely unclear how strongly an siRNA needs to be bound in a successful polyplex based delivery agent.

In addition to size and size distribution, the charge ratio is often cited as an important parameter of a polyplex formulation (8,15,16). We maintain that, from a physicochemical point of view, both the density of cationic charges and their relative spatial distribution should be important, and investigations into the binding of nucleic acids in polyplexes displaying a variegation of these parameters should give important clues as to their suitability for further transfection studies *in vitro*, and, in the long run, *in vivo* (3).

Many studies on siRNA complexation and release from polyplexes aim at optimizing single parameters in an otherwise homologous series of materials. Such parameters include *e.g.* the polyethylene glycol (PEG) content of PAMAM (4), the number of cationic amine functions in PVAs (6), the length of arginine-rich peptides (8), the molecular mass of branched PEI (10), and the grafting of PLL brushes (7). In contrast, studies which compare strongly diverging classes of complexing agents are relatively rare: Among these are a comparison between siRNA complexes with PLL and PAMAM (17), as well as cellular uptake studies of siRNA complexes with - among others - bPEI, and commercial lipid based agents (18). Biophysical parameters of polyplexes with small RNA and PEI, Chitosan and poly(allylamine) were characterized in a comparative fashion (12). The influence of polyplex stability on transfection efficiency was tested by

comparing two polymers with different charge density, a styrene derivative (QNPHOS) and pDMAEMA (14). Jensen *et al.* (19) compared *in vitro* gene silencing and toxicity of polymers, among them PAMAM and N-(2-hydroxypropyl) methacrylamide (HPMA).

Methods for Polyplex Characterization

As with the vast number of materials, there is a plethora of methods employed to characterize polyplexes, many of which employ fluorescence labels as reporter entities (18). In addition to conventional applications of fluorescence activated cell sorting (FACS) and confocal microcopy of siRNA cellular uptake (2,20), advanced techniques such as time resolved fluorescence spectroscopy (21) and fluorescence correlation spectroscopy (FCS) (11) have been applied to study labeled nucleic acids in polyplexes during formulation (11), in biological fluids (22), during cellular uptake and intracellular release (23). In addition to polyplex stability, the integrity of the cargo (siRNA, plasmid DNA or ODN) is accessible *via* Förster resonance energy transfer (FRET), which necessitates labeling of the nucleic acid with a FRET dye pair. Nuclease resistance of ODN complexes was tested by determination of the R/G ratio (24), based on a setup first described by Uchiyama *et al.* (25). siRNA integrity in liposomes was measured with dual color FCS (26).

Goal of this Work

Here, in a step towards characterizing optimal complexation and release properties of siRNA polyplexes, we have investigated a variety of structurally and chemically diverse nanoscale polyplexes (see schemes in Fig. 1 and characterization data in Supplementary Table SI), comparing them in various assays which highlight different aspects of siRNA binding to cationic compounds. In continuation of our previous work, we have based the assays on fluorescence, and encountered a strong dependence of fluorophore brightness on complexation or release from a polyplex. We identify microscale thermophoresis as a fast method to characterize polyplex formation under equilibrium conditions, and develop a nuclease protection assay based on FRET labeled siRNA to characterize the kinetics of siRNA release from polyplexes. Degradation kinetics offer clues to the existence of multiple populations of siRNA with differential accessibility within a formulation.

MATERIALS AND METHODS

Nanoparticles

The set of nanoparticles (see Fig. 1) consisted of a poly-L-lysine brush (*i.e.* a cylindrical polymer with densely grafted poly-L-lysine side chains) (27), an HPMA based block copolymer (consisting of the statistical copolymer N-(2-hydroxypropyl) methacrylamide-s-N-(3-aminopropyl) methacrylamide and a short terminal 3-guanidinopropyl methacrylamide block, (HPMA-s-APMA)-b-GPMA) (28), a cationic peptide (26 residues, enriched in histidine) (29), a cationic lipid (Oligofectamine™ Reagent, Invitrogen, LifeTechnolgies, Carlsbad, USA), a nanohydrogel (preformed particles consisting of a pegylated outer shell and an inner core containing spermines) (30,31) and a manganese oxide (MnO@SiO2) particle (consisting of a manganese oxide core covered with silica and surface modified to contain a cationic amine layer) (32). Knockdown experiments with HPMA based block copolymers, nanohydrogels and $MnO@SiO_2$ particles were performed with a second batch synthesis.

siRNA

All experiments were carried out with an siRNA directed against GFP messenger RNA (sense strand: 5′-GCAAGC UGACCCUGAAGUUCAU-3′, antisense strand: 5′-GAAC UUCAGGGUCAGCUUGCCG-3′) obtained from IBA (Göttingen, Germany). siRNA was purified by size exclusion chromatography (SEC), except for the nuclease resistance assay. In this case, the calibration compensated for a slight presence of free donor dye. For formation and stability assays, the siRNA was labeled with Alexa Fluor 555 on the 3′ of the sense and ATTO 647N on the 5′ of the antisense strand. For *in vitro* uptake quantification and determination of intracellular integrity, the siRNA was labeled with Atto 488 on the 3′ of the sense and ATTO 590 on the 5′ of the antisense strand. For knockdown experiments, unlabeled anti GFP siRNA (IBA) and a negative control siRNA (sense strand 5′-AGGUAG UGUAAUCGCCUUGdTdT-3′, antisense strand 5′-CAAG GCGAUUACACUACCUdTdT-3′, Microsynth, Balgach, Switzerland) was employed.

Emission Profile of siRNA and Polyplexes

Emission profiles were recorded on a FP-6500 Fluorimeter (JASCO, Tokyo, Japan) equipped with an ETC-273T temperature controller and a HAAKE WKL26 cooling unit (ThermoFisher Scientific) in a 15 µl quartz glass cuvette (Hellma, Müllheim, Germany) for 1 µM siRNA complex solutions (25 pmol siRNA in 25 µl 1x phosphate buffered saline) (1x PBS; pH 7.4, 140 mM NaCl, 2.7 mM KCl, 1.5 mM KH_2PO_4, and 8.06 mM Na_2HPO_4) at donor excitation (543 nm) and acceptor excitation (633 nm) with spectral correction for PMT (emission) and illumination lamp (excitation) with donor emission analyzed at 565 nm and acceptor emission at 665 nm at 1 nm datapitch and a bandwidth of 3 nm for excitation and emission.

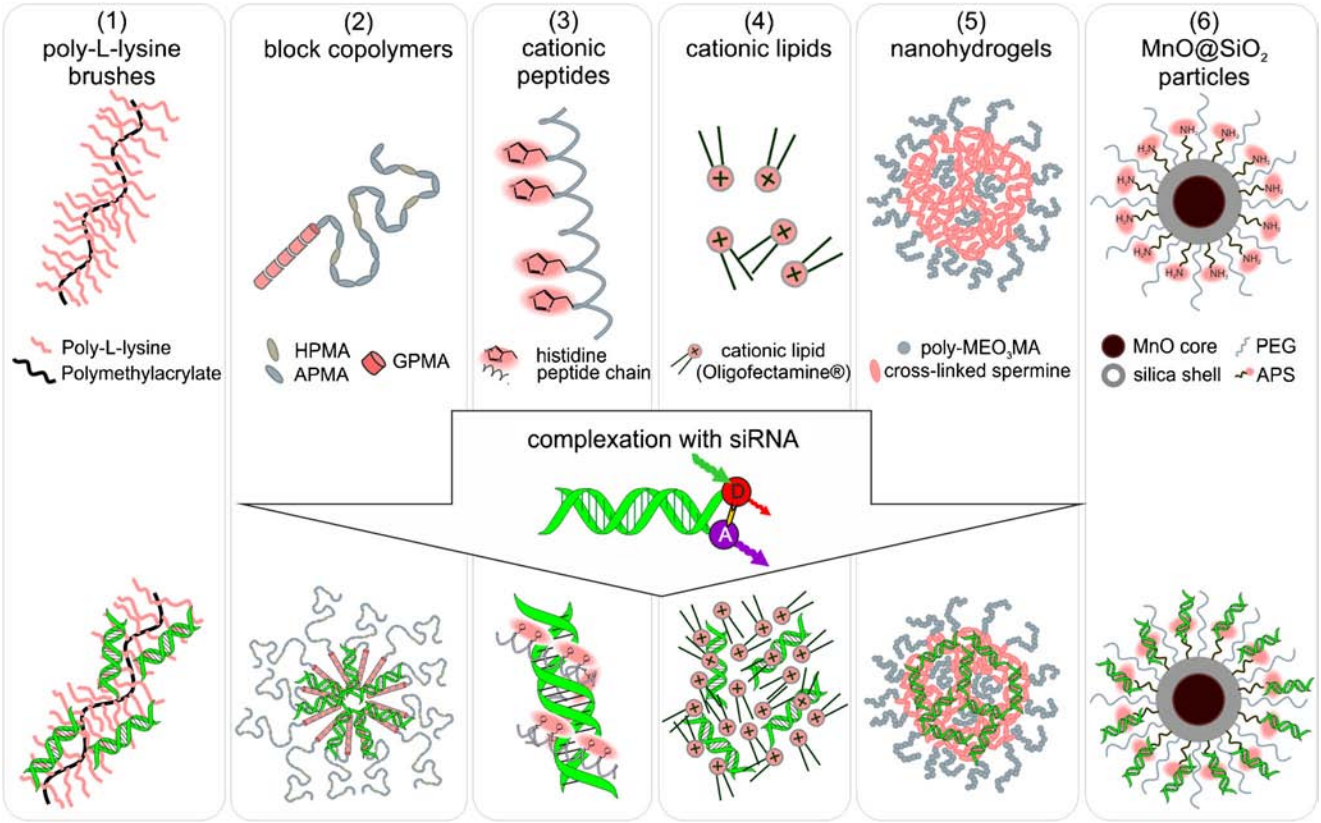

Fig. 1 Different types of cationic carrier systems under investigation. Poly-L-lysine brushes (1), HPMA based block copolymers (2), cationic peptides (3), Oligofectamine™ (4), nanohydrogels (5) and MnO@SiO_2 particles (6) are displayed as precursors without siRNA and as polyplexes with siRNA.

Electrophoretic Mobility Shift Assay (EMSA)

Ten picomole of siRNA was incubated with the particle at various mass/mass (m/m) ratios in 20 µl 1xPBS for 20 min at room temperature, resulting in an siRNA concentration of 0.5 µM. Samples were loaded in the middle of a 1% agarose (1xTBE running buffer) gel which was run at 120 V for 50 min. The gel was analyzed with the Typhoon 9600 (GE Healthcare, Buckinghamshire, UK) at 532 nm excitation wavelength and 580BP30 (donor signal) and 670BP30 emission filter (FRET signal) as well as with 633 nm excitation and 670BP30 emission filter (acceptor signal). For data analysis the fluorescence signal of free siRNA (on the level of the siRNA only sample) of the acceptor signal was quantified and expressed as percentage of the fluorescence signal of the whole lane. Obtained data was fitted *via* a five parametric dose response curve (Graph Pad prism) resulting in a value for 50% binding (BR_{50}).

Thermophoresis

For determination of BR_{50} values, complexes were prepared by serial dilution of the particle in 1xPBS at 16 different m/m ratios ranging from 700 to 0.02 and addition of siRNA solution leading to a final siRNA concentration of 50 nM (1 pmol in 20 µl) in each sample. Samples were incubated for 20 min and loaded into Monolith™ NT.115 standard treated capillaries (K002). Samples were measured with a Monolith NT.115 (Nanotemper, Munich, Germany) using red excitation and emission with 100% LED and 20% MST power. Each measurement was repeated five times with 5 s equilibration, 30 s Laser-On and 5 s decay time. An EC_{50} value was obtained with the NT Analysis software on a Hot/Cold evaluation employing a Hill fit. EC_{50} values were interpreted as BR_{50} values.

For determination of heparin release, 8 aliquots of complex solution at the respective m/m (200 nM siRNA) were prepared and incubated for 20 min. Heparin was added to each aliquot at a different z^-_{Hep}/z^-_{RNA} ratio. Final concentration of siRNA was 100 nM (2 pmol in 20 µl). After 30 min incubation samples were analyzed as mentioned above.

Heparin Competition Assay

Complexes were preformed at two different m/m ratios in 1xPBS and aliquoted in samples containing 5 pmol siRNA in 20 µl (0.25 µM) each. To each aliquot, heparin (Biochrom AG) at a different z^-_{Hep}/z^-_{RNA} (amount of negative charges

of heparin per amount of negative charges of siRNA) ratio was added. The z^-_{Hep}/z^-_{RNA} was calculated under the approximation that 200 g heparin and 340 g siRNA each contain 1 mol negative charges. The mixtures were incubated for 30 min and loaded on a 1% agarose gel. The gel was run at 120 V for 50 min and detected as described above.

Quantification was carried out as described for the EMSA analysis.

Nuclease Resistance Assay

Complexes were preformed at the respective m/m ratio in 1xPBS (1 μM siRNA, 10 pmol in 10 μl). After dilution with degradation buffer to achieve final reaction conditions of 40 mM Tris-HCl, 40 mM NaCl and 10 mM $MgCl_2$, 19 μl of complex solution (0.5 μM siRNA) was analyzed by recording emission profiles at donor excitation right before and after the addition of 1 μl of RNase V1 (20 mU of a 20 mU/μl solution, Invitrogen, Carlsbad, USA) over a period of 2 h, with measuring at various time points after the addition of the RNase. The R/G ratio at each timepoint was calculated from corrected spectral data as a ratio of acceptor emission to donor emission and used to calculate the integrity level on basis of the calibrated R/G system (see Supplementary Materials). Free siRNA was incubated under the same reaction conditions and used for normalization and comparison of data from experiments on different days (for the detailed analysis procedure see Supplementary Materials).

Serum Stability Assay

Complexes were preformed in 1xPBS at 1 μM siRNA. Complexes or free siRNA were mixed with 100% FBS (Invitrogen, Carlsbad, USA) in equal volumes to determine serum stability resulting in final 50% FBS and 0.5 μM siRNA. After the addition of the FBS the emission profiles at donor excitation were recorded over a period of 12 h, with measuring at various time points. For the 10% FBS sample a solution containing 20% FBS in PBS was used instead of FBS only, resulting in final 10% FBS. The R/G ratio at each timepoint was calculated as described for the nuclease resistance assay. Free siRNA was incubated under the same reaction conditions and used for normalization as described before.

Determination of Cellular Uptake

One day prior to transfection, 4×10^5 HeLa cells were seeded in 1 ml DMEM (Invitrogen, Carlsbad, USA) with 10% fetal bovine serum (FBS, Invitrogen) in 24-well tissue culture treated plates. At the time of transfection, medium was replaced by 185 μl DMEM. Polyplexes were prepared in OptiMem (Invitrogen) at cc_1 with 31 pmol siRNA in a volume of 65 μl. After 20 min maturation time, they were added dropwise to the wells resulting in a final siRNA concentration of 125 nM. 4 h after transfection, the medium was replaced by DMEM with 10% FBS. After 20 h, cells were washed with PBS, 0.2 mg/mL heparin solution and again PBS. For lysis, cells were incubated on ice for 30~min in 150 μl PBS containing 2% SDS and 1% TritonX. Cell debris was removed by centrifugation at 16000×*g* and 4°C for 20 min. 50 μl of lysate was transferred to black 96 well plates and acceptor fluorescence measured on an Infinite M200 Pro (Tecan, Austria) at 561 nm excitation and 610 nm emission. Calibration was carried out by diluting siRNA at various concentrations in cell lysate of untransfected cells. Fluorescence values were normalized to protein content by submitting another 50 μl of lysate to the ROTI^{TM} Quant universal assay according to the manufacturer's instructions. All data result from biological triplicates each done in technical duplicates.

Determination of Intracellular siRNA Integrity

The same transfection protocol as carried out for uptake quantification was repeated. After the washing steps, cells were trypsinized and resuspended in PBS. Cells were analyzed on a LSR-FortessaSORP in the donor (Ex 488 nm, 530BP30 emission filter) and FRET (Ex488 nm, 670BP30 emission filter) channels with the FRET channel compensated for bleedthrough of donor and acceptor fluorophores. Data was evaluated with FlowJo Software (TreeStar Inc, USA). For R/G calculation, the ratio of FRET to donor fluorescence intensity for each cell was derived as a new parameter and its median dessignated as R/G value. All data result from biological triplicates each done in technical duplicates.

Size Determination by FCS

Fluorescence correlation spectroscopy (FCS) was performed using an FCS setup (Zeiss, Oberkochen, Germany) consisting of the module ConfoCor2 and an inverted microscope model Axiovert 200 with a Zeiss C-Apochromat 40x/1.2 W water immersion objective. The acceptor fluorophore was excited by a Helium Neon laser (633 nm) and the emission was collected after filtering by a LP650 long pass filter. For detection, an avalanche photodiode that enables single-photon counting was used.

Samples were prepared analogously to the EMSA assays at a 0.5 μM siRNA concentration and allowed to mature for 20 min. Brushes were measured undiluted, the five other complexes were further diluted in PBS to a final concentration of 50 nM siRNA . Samples were transferred to an eight-well polystyrene chambered cover glass (Laboratory-Tek, NalgeNunc International) for the measurement.

Knockdown Experiments

One day prior to transfection, 4×10^5 HeLa MAZ ODC cells (33) were seeded in 1 ml DMEM (Invitrogen, Carlsbad, USA) with 10% fetal bovine serum (FBS, Invitrogen) in 24-well tissue culture treated plates. At the time of transfection, medium was replaced by 185 µl DMEM. Polyplexes were prepared in OptiMem (Invitrogen) at cc_1 with 16 pmol siRNA in a volume of 65 µl. After 20 min maturation time, they were added dropwise to the wells resulting in a final siRNA concentration of 62.5 nM. 4 h after transfection, the medium was replaced by DMEM with 10% FBS. After 20 h, cells were incubated with fresh medium containing 2 µM MG115 (Sigma Aldrich, Germany) for another 5 h. For analysis, cells were washed with PBS, trypsinized, resuspended in PBS and measured on a LSR-FortessaSORP, BD, Heidelberg, Germany, at 488 nm excitation with a 530BP30 filter (GFP signal). Data was evaluated with FlowJo Software. GFP signal was calculated as the product of the percentage of GFP positive cells and their median fluorescence intensity compared to the value of an only MG115 treated control. All data result from biological triplicates each done in technical duplicate.

RESULTS

In order to develop a sequence of assays suitable to characterize the differential kinetic stability of variegated siRNA polyplexes, a panel of cationic reagents was established (see schemes in Fig. 1 and characterization data in Supplemental Table SI), which are currently being intensively scrutinized for their performance as nucleic acid delivery agents in cell culture, and, in some cases, for potential *in vivo* applications. The panel included poly-L-lysine brushes (27), HPMA based block copolymers (28), cationic peptides containing a lysosomal release sequence (29), the cationic lipid Oligofectamine™, a commercial and widely used standard in cell culture transfections (2,20), nanohydrogels (30,31) and nanoparticles consisting of a manganese oxide core covered with silica and surface modified to contain a cationic amine layer (32). All particles were synthesized as previously described. The nanoparticular carriers are formed in cases (Fig. 1 1–4) by polyplex formation with siRNA. In contrasting cases (Fig. 1 5,6), however, the siRNA is condensed onto preformed nanoparticles. To our knowledge, this panel represents a so far unpreceeded structural variety in comparative studies of siRNA polyplexes (14,17–19).

Fluorescence Properties of FRET Labeled siRNA Strongly Depend on Polyplex Structure

This study employs an siRNA which is labeled with two fluorophores forming an efficient FRET pair. Its fluorescent properties including the FRET characteristics have previously been optimized (34) and the FRET-labeled siRNA was shown to be biologically active when delivered as standard lipoplex formulations in RNAi studies using EGFP as reporter gene (35). In addition to efficient detection of siRNA molecules during formulation, determination of the ratio of acceptor and donor fluorescence (R/G ratio) upon donor excitation allows calculation of integrity levels, and thus to rapidly identify and avoid formulation steps that result in RNA degradation (36). The standard procedure for the formulation of fluorescently labeled siRNA in polyplexes started from a 5 µM stock solution of double-stranded, FRET labeled siRNA (35) in PBS, to which the various nanoparticles or precursors thereof were added at room temperature. Assays were conducted after a maturation period of 20 min.

During the establishment of this protocol, we noticed that fluorescence intensity changed significantly during complexation in the cuvette, and the changes varied depending on the type of polyplex formed. Figure 2a1 and a2 show fluorescence spectra upon donor and acceptor excitation respectively of a 1 µM solution of siRNA alone or in the presence of either the HPMA based block copolymers or branched poly-L-lysine brushes. Formulation of siRNA results in a strong reduction of fluorescence intensity by a factor of 12 and 17 for poly-L-lysine brushes and HPMA based block copolymers, respectively. This effect was replicated with siRNA carrying different fluorescent labels (Supplemental Fig. S1), showing that the effect is not restricted to the specific structure of the fluorophores used in the FRET labeled siRNA.

Upon addition of heparin in concentrations sufficient to release the siRNA from the polyplexes by anion competition (*vide infra*), the fluorescence is nearly fully recovered (Fig. 2b1 and b2), including an R/G ratio of 24, which corresponds to fully intact siRNA. This indicates that the observed effect is reversible and not related to RNA degradation, precipitation, or loss of fluorophores. To relate the extent of quenching to conventional Stern Volmer type quenching (37), siRNA fluorescence was measured as a function of salt concentrations up to 1 M, yielding a maximum quenching factor of 7 fold for 1 M NaCl, and weaker effects for NaBr and L-lysine (4 fold and 2 fold, respectively) (Supplemental Fig. S2).

While some part of this observation may be explained with self quenching and an inner filter effect of the locally

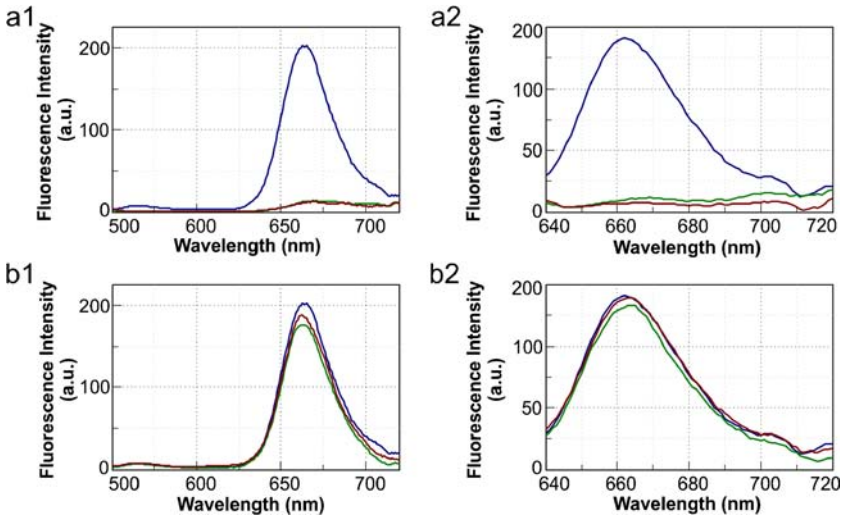

Fig. 2 Fluorescence quenching of poly-L-lysine brushes and HPMA based block copolymers. Emission spectra of 1 μM siRNA only (*blue*), brushes at m/m 2/1 (*green*) and block copolymers (*red*) at m/m 100/1 before (a1 at donor, a2 at acceptor exCitation) and after (b1 at donor, b2 at acceptor exCitation) addition of heparin at z^-_{Hep}/z^-_{RNA} 20.

concentrated fluorophores (11,38), the properties of the various compounds clearly exert a dominant influence. This is evident from the wide range of fluorescence intensity changes listed in Table I, which even includes a 3-fold fluorescence boost in the case of nanohydrogels.

Tracing the Formulation of siRNA into Polyplexes by EMSA

To establish a basis for comparative analysis of these structurally very diverse cationic compounds, each was formulated with FRET-labeled siRNA at different $mass^{Particle}/mass^{siRNA}$ (m/m) ratios. Cationic compounds were incubated with siRNA for 20 min in PBS and submitted to an electrophoretic mobility shift assay (EMSA), which is well established in the field (2,14,29). Forming the polyplexes directly in PBS was chosen in order to directly characterize the polyplexes under an ionic strength comparable to a physiological setting, as each transfer from one medium to another bears the possibility of changing the physic-chemical characteristics of a polyplex (4). However, since literature features numerous instances where polyplex formation was conducted in low ionic strength conditions, we have verified for one class of polyplexes, namely those originating from cationic peptides, that binding characteristics do not significantly differ between high and low ionic strength conditions (Supplemental Fig. S3). In a typical experiment, a constant amount of siRNA was titrated with increasing amounts of particle, and an effective value for 50% binding of siRNA to the delivery compound (BR_{50}) was determined. We furthermore determined the two lowest values at which complexation was apparently exceeding 95%, designated as "cc_1" und "cc_2" values. Figure 3 shows the EMSA data for formulations of the six cationic compounds, and key values are summarized in Table II.

Table I Fluorescence Intensity of siRNA in Polyplexes

Nanoparticle	Fluorescence intensity [%][a] at cc_1[b]	at cc_2[c]
Lysine brushes	7	11
Block copolymers	5	12
Peptides	101	125
Lipids	41	46
Nanohydrogels	234	290
MnO@SiO_2 particles	72	63

[a] Acceptor signal in polyplexes normalized to siRNA only

[b] the lowest mass/mass ratio at which complexation exceeds 95%

[c] the second lowest mass/mass ratio at which complexation exceeds 95%

Visual inspection of the electrophoresis experiments in Fig. 3 already indicates, that the different compounds exhibit variegated properties, in particular with respect to the stability of the resulting polyplexes. Thus, while in all experiments the lower band of free siRNA eventually disappears at increased concentrations of cationic compound, nanohydrogels and manganese oxide particles display a broad smear between free siRNA band and pocket (Fig. 3a5 and a6), which reflects siRNA that has dissociated from the polyplexes during electrophoresis. This allows to conclude an increased off-rate of siRNA from the polyplexes, as compared to the other formulations, in which the siRNA stays firmly complexed in the loading pockets and only small amounts of less tightly bound siRNA can be seen as weak smear (Fig. 3a1–4). The most abrupt transition from free to bound form is found with the poly-L-lysine brushes (Fig. 3a1), while with the manganese oxide particles (Fig. 3a6) all siRNA is released during electrophoresis to an extent that no siRNA remains in the pockets at cc_1 and cc_2 conditions. Of note, complexation of siRNA by brushes and block copolymers quenches fluorescence of both

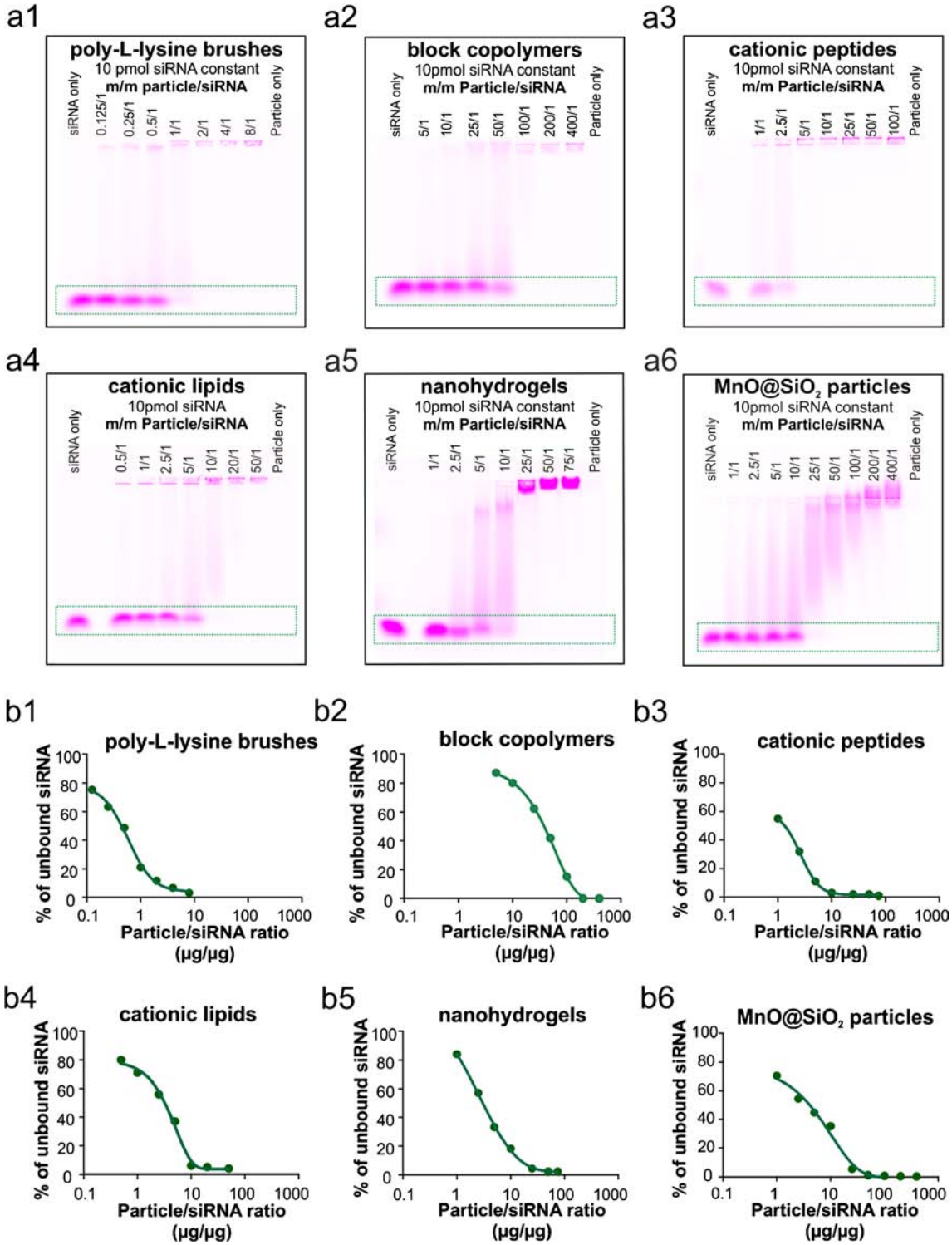

Fig. 3 EMSA analysis of polyplex formation. Complexation of siRNA with the panel of nanoparticles. poly-L-lysine brushes (1), block copolymers (2), cationic peptides (3), cationic lipids (4), nanohydrogels (5), $MnO@SiO_2$ particles (6). Several ratios of particle to siRNA (mass/mass ratio) passing the minimal ratio for complete complexation are loaded on an agarose gel (a1–6) and fluorescence signal of free siRNA (highlighted by green rectangle in a1–6) is quantified and fit with a 5 parametric dose response curve (b1–6).

attached fluorophores (see above), therefore the intensity observed of material remaining in the pockets is rather weak (Fig. 3a1 and a2).

Because of the abovementioned quenching, fluorescence signal in the binding pocket was not included in data interpretation. Two alternative ways of data

Table II Binding Ratios of Polyplexes

Nanoparticle	cc_1	cc_2	BR_{50}[a] value for EMSA	BR_{50}[a] value for MST
Lysine brushes	2/1	4/1	0.6	0.6 (0.5[b])
Block copolymers	100/1	200/1	43.8	50.4 (55.0[b])
Peptides	5/1	10/1	2.5	2.5
Lipids	10/1	20/1	4.1	7.1
Nanohydrogels	25/1	50/1	1.8	14.6
$MnO@SiO_2$ particles	25/1	50/1	7.3	118

[a] mass/mass ratio at which 50% of siRNA is bound

[b] BR_{50} value from fluorimetric titration curve

evaluations were considered, namely (i) quantifying only the signal of free, *i.e.* uncomplexed siRNA (identified by comparison with control lane), or (ii) also taking into account the smear visible between the signal of free siRNA and the pocket (see Supplemental Fig. S4). As procedure (i) yielded the most rational results, we concluded that the smear in the lane can be considered as loosely bound siRNA that is extracted from the polyplex during the process of electrophoresis. Following this procedure (i) led to Fig. 3b1–6, which contains plots of the fractions of remaining free siRNA as a function of the mass ratio for each compound. From this and the values in Table II it is readily apparent that the mass ratios for complexation differ strongly, presumably reflecting the charge density of a given compound: values for BR_{50} as well as cc_1 and cc_2 values differ up to 50 fold. Further analysis shows, that the slopes which define the transition from beginning to complete complexation differ among the compounds as well. Although this type of analysis is clearly inadequate for the deduction of detailed parameters such as a Hill coefficient, we contend that some aspects of cooperative binding are being reflected.

Judged altogether, poly-lysine brushes appear to bind most tightly, closely followed by block copolymers, cationic peptides and lipids. The nanohydrogels show a lower binding ratio for 50% binding, but a significant off-rate as evidenced by siRNA released in the time span of the experiment. The manganese oxide particles display the weakest binding. However, the non-equilibrium conditions, under which the analysis was conducted, are liable to exert a negative influence on binding. Thus, the electrical field applied during electrophoresis, as well as the buffer might both be detrimental to binding, as strongly suggested by the aforementioned smear. Alternative methods are therefore warranted, which eschew inflexible buffer conditions and the detrimental effects of strong electric fields.

Characterization of Polyplex Formation by Thermophoresis

In addition to characterization by the classical EMSA, we explored MST, a method based on differential migration behavior in a thermal gradient. We found that this method yields binding curves with minimal amounts of fluorescent molecules in a short time span. Briefly, polyplexes were prepared by a 16 step serial dilution of 30 μg of the delivery compound followed by complexation with a constant amount of siRNA (each 1 pmol or 14 ng). This amounts to around 250 ng of labeled siRNA and 30 μg of delivery compound for a full analysis. 20 min after complexation, samples were analyzed as detailed in the method section. In our hands, the method yielded reproducible binding curves for most compounds within 1 h, from which a fit (Fig. 4) allows for determination of a half-maximal complexation point. It is apparent from the data shown in Fig. 4 (compare inlays) that the quality of the primary binding curves, which were obtained with the same type of standard capillary for better comparison, is somewhat variable among the different types of polyplexes. Apparently, the quality mostly depended on polyplex adhesion to capillary walls, and with little effort some improvement is possible at moderate increase in turnaround time.

The resulting values are compiled in Table II. Interestingly, the BR_{50} values largely correspond to those obtained by EMSA for those compounds, which do not show any smear in the EMSA, the poly-L-lysine brushes, block copolymers, peptides and lipids (Fig. 3a1–4). On the other hand, the values differed markedly for nanohydrogels and manganese oxide particles (Fig. 3a5 and 6), both of which are difficult to characterize by EMSA as a consequence of the high off-rate discussed above as smearing. The fluorescence quenching effect observed for brushes and block copolymers has significant bearings for the MST experiments, since it superimposes to changes of fluorescence as a consequence of thermophoresis. For the strongly quenching poly-L-lysine brushes and block copolymers it essentially blots out the latter. Thus, the measurements are comparable to a binding curve from a conventional fluorimetric titration. Some actual examples for such a titration are shown in Supplemental Fig. S5, and yield BR_{50} values comparable to the ones obtained from the MST experiments (Table II).

In summary, we established MST as a suitable method to characterize binding of labeled siRNA in polyplexes. The determined relative order of binding among the polyplexes is similar to EMSA experiments and for strong binders the method produces similar

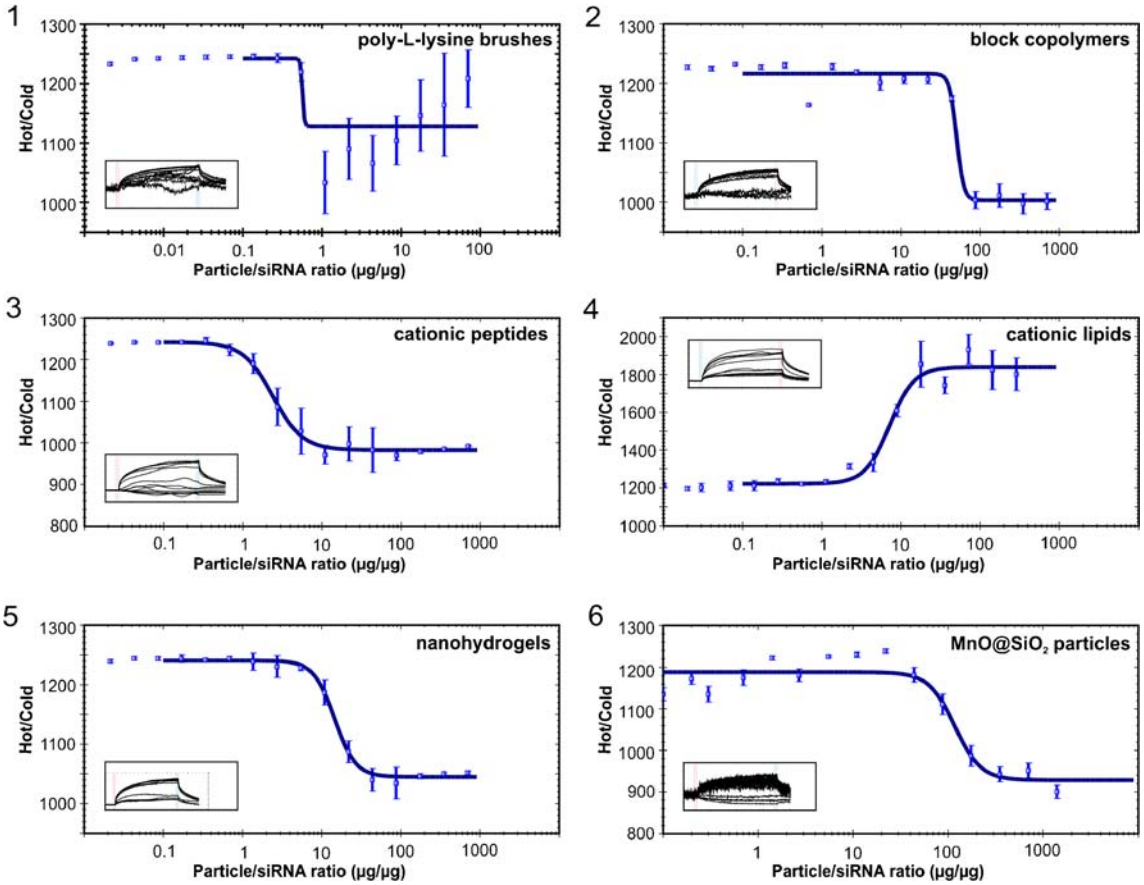

Fig. 4 Thermophoretic analysis of polyplex formation. Hot-cold mode evaluation and Hill fit of polyplexes titrated from m/m 0.02 to 700 ($n = 5$). poly-L-lysine brushes (1), block copolymers (2), cationic peptides (3), cationic lipids (4), nanohydrogels (5), $MnO@SiO_2$ particles (6). The inlays depict the primary binding curves of one measurement series.

ratios for 50% binding. However, for binders with significant off-rates, those values differ. This can be rationalized because MST measurements are conducted under equilibrium conditions, whereas during electrophoresis, siRNA is removed from the binding equilibrium. In case of weak binding affinities, siRNA is permanently released from the complex, resulting in the observed smear during EMSA, whereas in MST the steady state conditions allow re-binding and thus lead to higher particle binding rates. One particular advantage of MST over EMSA is the possibility to use a wide range of buffers, including various salt conditions, whereas EMSA is essentially restricted to TBE and related buffers, which are remote from physiological conditions.

Release of siRNA from Polyplexes in Heparin Competition

The differential behavior of the weakly binding nanohydrogels and manganese oxide particles between EMSA and MST analysis warranted a more exact comparative characterization of the siRNA release from the polyplexes. In following established heparin competition protocols (8,12), samples from conditions cc_1 and cc_2 were incubated with increasing amounts of heparin, and again subjected to EMSA. The z^-_{Hep}/z^-_{RNA} ratio (amount of negative charges of heparin per amount of negative charges of siRNA) was expected to characterize the strength of siRNA binding in a setting of competing negative charges. However, as shown in Fig. 5 and compiled in Table III, all z^-_{Hep}/z^-_{RNA} values are close to 2.5 and 5, for the cc_1 and cc_2 polyplex composition, respectively. This is an interesting piece of data since it seems to universally apply to all compounds, but offers

Fig. 5 Release of siRNA studied by heparin competition. EMSA analysis and thermophoresis for determination of z^-_{Hep}/z^-_{RNA} values for release from complexes at cc_1 and cc_2 of poly-L-lysine brushes (1), block copolymers (2), cationic peptides (3), cationic lipids (4), nanohydrogels (5), $MnO@SiO_2$ particles (6). EMSA (a1–6), fluorescence signal of free siRNA quantified and fit with a 5 parametric dose response curve (b1–6) and analysis by thermophoresis (c1–6).

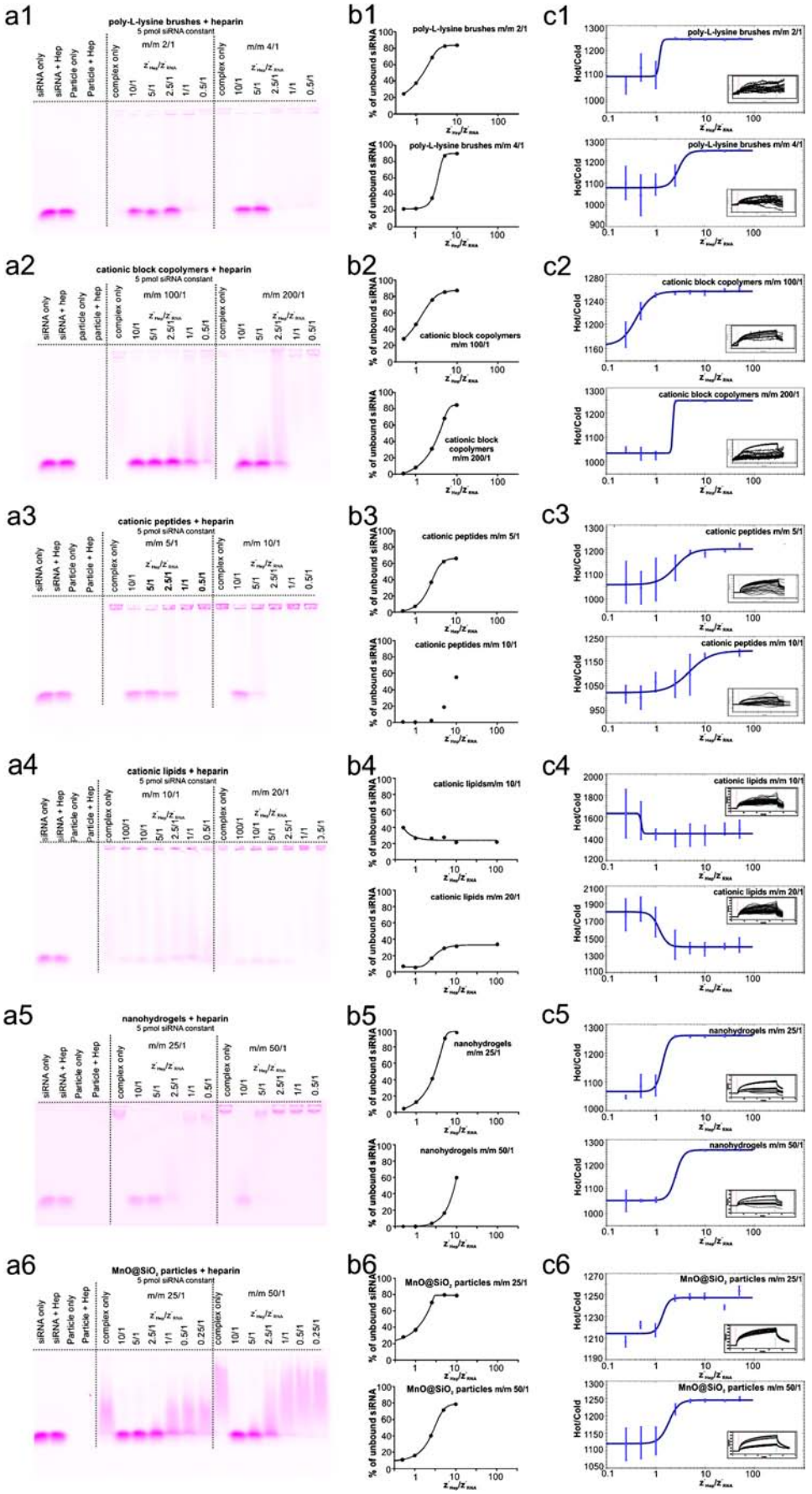
a1
poly-L-lysine brushes + heparin
5 pmol siRNA constant
siRNA only
siRNA + Hep
Particle only
Particle + Hep
complex only
m/m 2/1
m/m 4/1
b1
poly-L-lysine brushes m/m 2/1
poly-L-lysine brushes m/m 4/1
% of unbound siRNA
c1
poly-L-lysine brushes m/m 2/1
poly-L-lysine brushes m/m 4/1
Hot/Cold
a2
cationic block copolymers + heparin
5 pmol siRNA constant
m/m 100/1
m/m 200/1
b2
cationic block copolymers m/m 100/1
cationic block copolymers m/m 200/1
c2
cationic block copolymers m/m 100/1
cationic block copolymers m/m 200/1
a3
cationic peptides + heparin
5 pmol siRNA constant
m/m 5/1
m/m 10/1
b3
cationic peptides m/m 5/1
cationic peptides m/m 10/1
c3
cationic peptides m/m 5/1
cationic peptides m/m 10/1
a4
cationic lipids + heparin
5 pmol siRNA constant
m/m 10/1
m/m 20/1
b4
cationic lipidsm/m 10/1
cationic lipids m/m 20/1
c4
cationic lipids m/m 10/1
cationic lipids m/m 20/1
a5
nanohydrogels + heparin
5 pmol siRNA constant
m/m 25/1
m/m 50/1
b5
nanohydrogels m/m 25/1
nanohydrogels m/m 50/1
c5
nanohydrogels m/m 25/1
nanohydrogels m/m 50/1
a6
MnO@SiO2 particles + heparin
5 pmol siRNA constant
m/m 25/1
m/m 50/1
b6
MnO@SiO2 particles m/m 25/1
MnO@SiO2 particles m/m 50/1
c6
MnO@SiO2 particles m/m 25/1
MnO@SiO2 particles m/m 50/1

Table III z^-_{Hep}/z^-_{RNA} Values for Heparin Release

Nanoparticle	z^-_{Hep}/z^-_{RNA} values for cc_1			z^-_{Hep}/z^-_{RNA} values cc_2		
	Complete release[a]	$EMSA_{50\%}$[b]	$MST_{50\%}$[c]	Complete release[a]	$EMSA_{50\%}$[b]	$MST_{50\%}$[c]
Lysine brushes	2.5	1.3	1.2	5	3.3	2.8
Block copolymers	2.5	1.1	0.4	5	3.0	2.2
Peptides	5	2.3	2.5	10	n.a.	4.9
Lipids	n.a.	~ 0.5	0.5	n.a.	2.8	1.2
Nanohydrogels	5	2.8	1.4	10	n.a.	2.5
MnO@SiO_2 particles	2.5	~1.6	1.4	5	2.7	1.8

[a] z^-_{Hep}/z^-_{RNA} ratio for complete release determined by EMSA

[b] z^-_{Hep}/z^-_{RNA} ratio for 50% release determined by EMSA

c z^-_{Hep}/z^-_{RNA} ratio for 50% release determined by MST

n.a. not available

very little discrimination as to the binding strength. One most interesting aspect is that release from cationic peptides as well as from cationic lipids could not be driven to completion even at increased heparin concentrations, indicating a subpopulation of siRNA in this formulation, which is kinetically inert to release by competition.

Nuclease Resistance Assay

In a further step, we aimed to characterize the fraction of siRNA that dissociates from polyplexes as part of a dynamic equilibrium. In tissue culture as well as in the bloodstream, loss of siRNA from polyplexes through dissociation is expected to be governed by competing ions, the binding constant, and the off-rate. The latter two determine the time of an siRNA spent unprotected in solution, during which it may undergo interactions with plasma proteins, including degradation by nucleases. To investigate this aspect, the polyplexes were challenged with nuclease at concentrations that completely degrade free siRNA within minutes (see Fig. 6a). The FRET-labeling of our model siRNA allows a fast and non-invasive surveillance of its integrity state throughout all steps of experimental manipulation. Upon addition of RNase V1 to a preparation of siRNA, the FRET effect, quantified *via* R/G ratio (20,34,39) decays along with siRNA integrity. In developing this effect into an assay, we have monitored the degradation of siRNA in polyplex formulations obtained at the cc_1 and cc_2 ratios of each of the six polyplex-forming compounds. R/G-time courses of individual polyplexes were obtained by real time monitoring of fluorescence intensities at the emission maxima of the dyes used for FRET labeling. From the R/G ratio, an integrity status was back-tracked using a calibration as previously described (34). As can be seen in Fig. 6b, the kinetics show characteristic behavior for each polyplex. The degradation kinetics of siRNA complexed with poly-L-lysine brushes and block copolymers require close attention, since the nearly quantitative quenching of fluorescence upon complexation results in reduced initial R/G ratios. This strongly skews the apparent integrity, thus prohibiting regular fitting of the data (Fig. 6b1 and b2). We have therefore used donor fluorescence as an alternative parameter. Degradation of the siRNA leads to a strong increase of donor fluorescence as a consequence of FRET breakdown, as can be seen in the control experiment with free siRNA. This signal, however, remains almost constant for brushes and copolymers, and we conclude that these particles warrant near complete protection against nuclease (see Supplemental Fig. S6). Cationic peptides and lipids (Fig. 6b3 and b4) still offer a significant degree of protection, while siRNAs complexed to nanohydrogels are rather quickly degraded (Fig. 6b5). Finally, the fast and nearly complete FRET decay observed for siRNA formulated to loosely binding manganese oxide particles (Fig. 6b6) comes closest to the kinetics of the free siRNA. An exponential decay model was fitted, based on the observed degradation rates, allowing to calculate mean lifetimes of the complexes under presented experimental conditions (see

Fig. 6 Nuclease resistance assay. Scheme of the nuclease resistance assay (**a**). Polyplexes at ratios cc_1 (*red* or *dark blue*), cc_2 (*orange* or *light blue*) and naked siRNA (*black*) were exposed to RNase V1 (b1–6) or to final 50% FBS (c1–6). Upon degradation of free or released siRNA, changes in FRET were used to determine siRNA integrity levels for the polyplexes over time. Data was used to fit a decay model. poly-L-lysine brushes (b1+c1), block copolymers (b2+c2), cationic peptides (b3+c3), cationic lipids (b4+c4), nanohydrogels (b5+c5), MnO@SiO_2 particles (b6+c6).

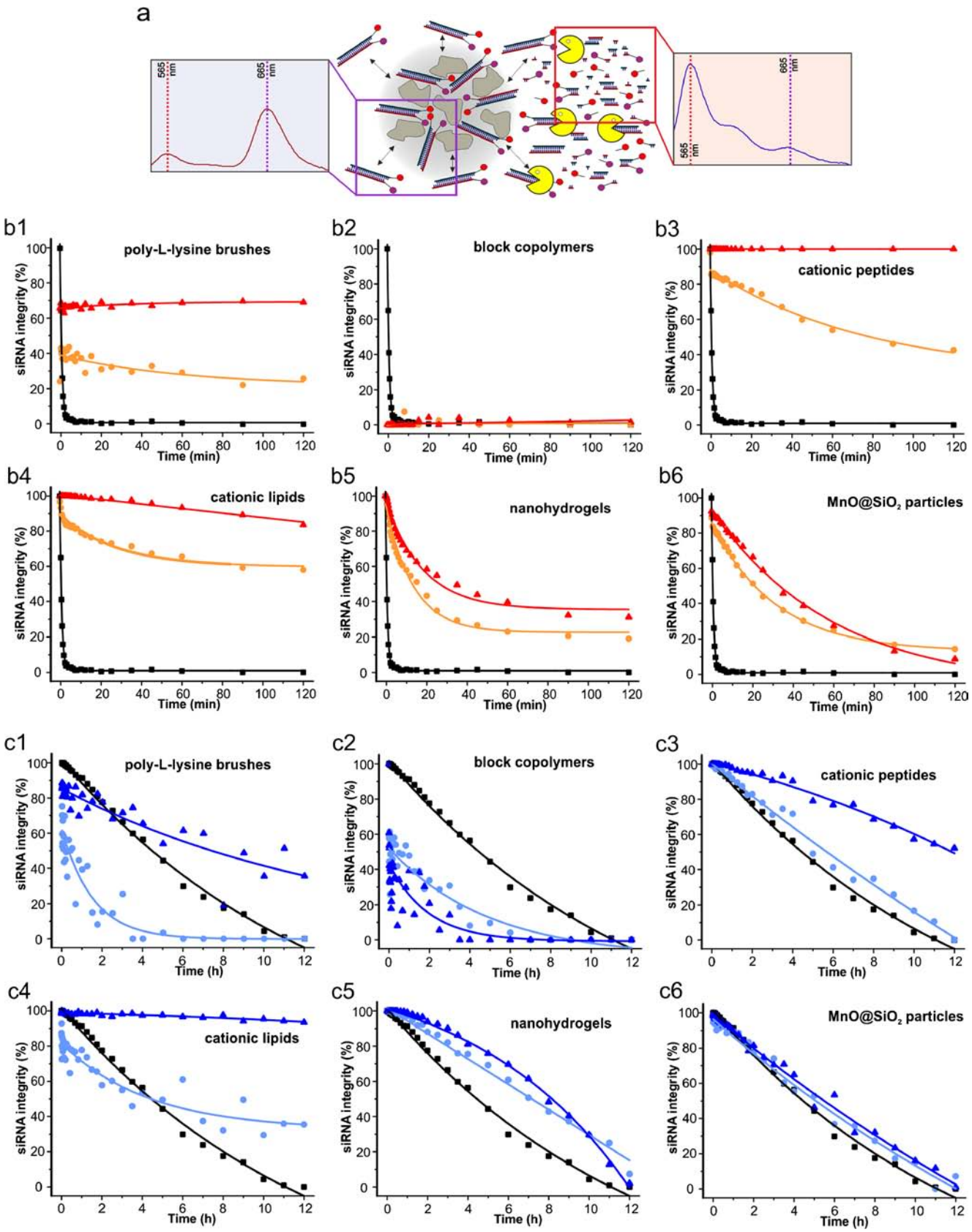

Table IV). Most interestingly, the kinetics of certain compounds could not be matched with a single exponential component fit, *e.g.* the nanohydrogels seem to contain at least two siRNA populations of strongly

Table IV Nuclease Resistance Assay

	cc_1		cc_2	
Nanoparticle	Mean lifetime[a]	Degradation time$_{20\%}$[b]	Mean lifetime[a]	Degradation time$_{20\%}$[b]
siRNA only	1 min	< 1 min	/	/
Lysine brushes	61 min	n.a.	n.a.	n.a.
Block copolymers	n.a.	n.a.	n.a.	n.a.
Peptides	78 min	11 min	> 2 h	> 2 h
Lipids	28 min	10 min	> 2 h	> 2 h
Nanohydrogels	13 min	3 min	18 min	6 min
MnO@SiO_2 particles	31 min	2 min	59 min	8 min

[a] mean lifetime of intact siRNA

[b] time after which 20% of siRNA is degraded

n.a. not available

diverging stability. Figure 6b5 clearly shows the degradation of nanohydrogel polyplexes leveling out at 30 and 40%, respectively, of intact siRNA even upon prolonged incubation, indicating an inaccessible population of siRNA in addition to the one that is quickly degraded.

Overall, this assay reproduces the order of binding strength previously derived by EMSA and thermophoresis quite well. Moreover, it offers more precise discrimination among compounds, whose properties were so far difficult to distinguish: Poly-L-lysine brushes and block copolymers display high stability, cationic peptides, and cationic lipids display intermediate stability towards nucleases.

siRNA Integrity in FBS Containing Medium

To assess conditions closer to *in vitro* RNAi assays and physiologic conditions, the FRET based siRNA integrity assay was applied to polyplexes in medium supplemented with FBS. Surprisingly, under typical cell culture conditions, including 10% FBS, degradation even of free siRNA was too slow, to allow discrimination of stability among various polyplexes (Supplemental Fig. S7). This emphasizes, that crucial siRNA degradation events do not take place in the serum outside cells during transfection experiments, and consequently, that relevant siRNA degradation takes place after cellular uptake. Significant siRNA degradation was observable only when the FBS content was increased to 50%, thus approaching conditions in the blood stream rather than in cell culture.

Figure 6c shows differential degradation kinetics for the various polyplexes at cc_1 and cc_2. As before, PLL brushes and block copolymers were evaluated *via* their donor signal due to the almost complete quenching (compare Supplemental Fig. S6). In particular the degradation characteristics of the cc_2 ratios largely reflected the order of binding strength previously derived from the nuclease digestion assay.

Intracellular siRNA Integrity

Ruling out instability of polyplexes in standard cell culture medium is highly suggestive that differences in intracellular integrity are a likely critical parameter for biological activity. To assess this feature, HeLa cells were transfected with the polyplexes at cc_1. At time points 4 h, 12 h and 24 h after transfection, cells were thoroughly washed with heparin, trypsinized to remove surface bound polyplexes, and submitted to analysis *via* flow cytometry. In analogy to R/G measurements in the cuvette, donor and FRET channel signals were used to derive an R/G ratio, which is displayed for three time points in Fig. 7. Signals from cells treated with MnO@SiO_2 particles were too weak for evaluation.

The presumed strong binders PLL brushes and block copolymers exhibited a very low intracellular R/G value, although it cannot be completely ruled out that quenching led to some bias in the evaluation. Cationic peptides, lipids and nanohydrogels display the highest intracellular integrity at 4 h. Interestingly, while lipids and peptides show a quick decrease in integrity levels around 12 h, integrity for nanohydrogels stayed relatively constant throughout the entire experiment.

Quantification of Cellular Uptake

In combination with intracellular integrity, siRNA uptake determines intracellular concentrations of siRNA potentially available for RNAi. To quantify uptake, HeLa cells were transfected with the polyplexes at cc_1 and intracellular siRNA content was assessed at three time points after transfection.

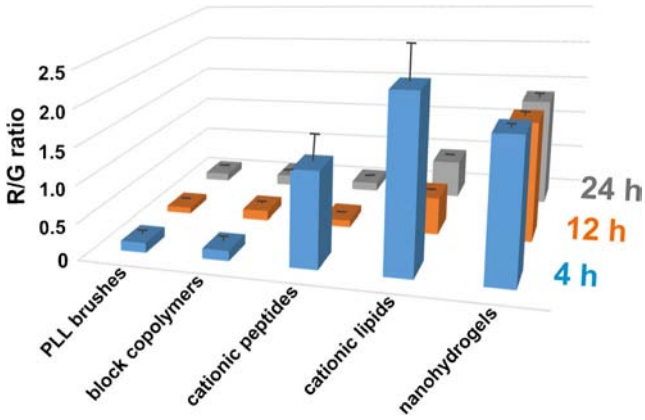

Fig. 7 siRNA integrity after cellular uptake assessed *via* an intracellular R/G. HeLa cells were transfected with the polyplexes at cc_1. 4 h (*blue bars*), 12 h (*orange bars*) and 24 h (*grey bars*) after transfection, cells were submitted to flow cytometry. By analyzing donor and FRET signal channels, an intracellular R/G ratio was derived.

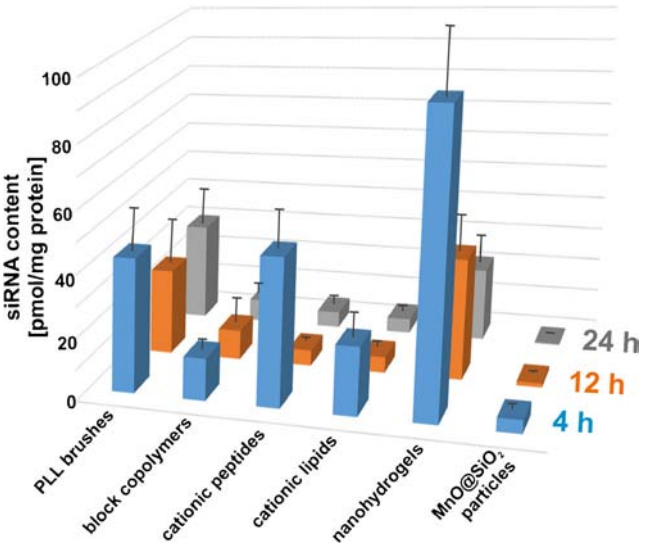

Fig. 8 Quantification of cellular uptake by siRNA fluorescence in cell lysate. HeLa cells were transfected with the polyplexes at cc_1. 4 h (*blue bars*), 12 h (*orange bars*) and 24 h (*grey bars*) after transfection, cells were lysed in Triton-X and SDS in order to allow a quantification of the siRNA, which is unbiased by intracellular location and effects deriving from the complexation. siRNA content is displayed as the fluorescence signal of the acceptor dye in cell lysate, normalized to protein content.

Cells were carefully washed with heparin to remove siRNA from polyplexes sticking on the cell surface, and then lysed in Triton-X and SDS. The latter was verified to be able to release siRNA from polyplexes, thereby avoiding quenching effects that may derive from intracellularly complexed siRNA (18).

The siRNA content, calculated from fluorescence intensities of the red acceptor dye in cell lysate, and normalized to protein content, is displayed in Fig. 8. The nanohydrogels showed the highest uptake, followed by cationic peptides and PLL brushes. Cationic lipids and block copolymers were taken up to a lower extent, while the $MnO@SiO_2$ particles displayed the weakest uptake. The time profiles showed a quick decrease in siRNA levels for peptides, lipids and nanohydrogels, while the level for the brushes remained largely high. The same was true for the copolymers, with the difference of their reduced initial level.

Knockdown Efficiency of Polyplexes Using GFP as Reporter Gene

All polyplex cc_1 formulations were tested in RNAi cell culture assays, using an *in vitro* reporter gene assay to evaluate the knockdown efficiency. HeLa cells expressing a destabilized GFP (33) were incubated with the polyplexes at 62.5 nM siRNA. After 24 h, cells were treated with a proteasome inhibitor for 5 h to boost the remaining GFP signal. Green fluorescence was read out by flow cytometry. As can be seen in Fig. 9, only the peptides and the lipids showed significant knockdown of 62% and 82% respectively, which is in agreement with literature on these two types of particles.

Size Determination

In a last step, polyplex size as a criterion concerning safe delivery and body clearance for a potential *in vivo* use (40) was assessed. The acceptor dye label of the siRNA enabled analysis by fluorescence correlation spectroscopy. Brushes, nanohydrogels and $MnO@SiO_2$ particles showed hydrodynamic radii of 60 nm, 22 nm and 18 nm respectively (see Tables V and SI). These values are similar to those determined for uncomplexed particles (27,30,32). Block copolymers also showed a monodisperse population with a peak size of 29 nm (28). Peptides and lipids showed strongly heterogenous aggregation, which is in accordance with published DLS measurements for the peptides (29).

DISCUSSION

In this work, we present a comparative characterization of the stability of a panel of structurally highly diverse polyplexes formed from dye labeled siRNA. We introduce MST, which has only recently been established in the life sciences (41) to the characterization of polymer and nanoparticles, where it has, to our knowledge, not yet been applied. While EMSA requires working in buffer systems compatible with electrophoresis, major advantages of MST over gel electrophoresis are free

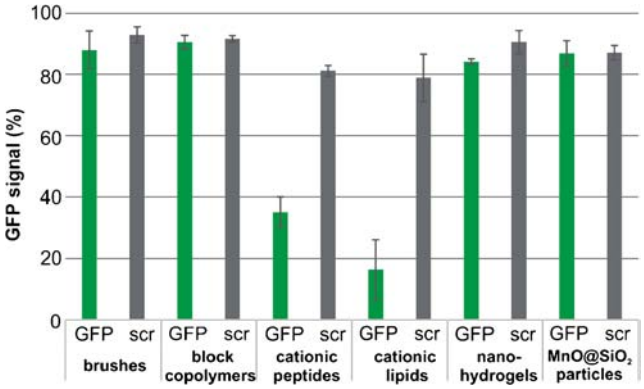

Fig. 9 Knockdown efficiency. HeLa cells expressing a destabilized GFP were incubated with the polyplexes at ratio cc_1 (siRNA 62.5 nM) for 24 h with anti GFP and scrambled siRNA, respectively, followed by incubation with a proteasome inhibitor for another 5 h. The GFP signal was read out by flow cytometry.

choice of buffer, and measurement under what are essentially equilibrium conditions. Hence, it stands to reasons that these two factors are the major causes for the disparate values, and thus thermophoresis appears better suited to reflect physiologically relevant conditions. The use of heparin in competition/release assays did reveal little information, except maybe that in case of the cylindrical brush polymers the z^-_{Hep}/z^-_{RNA} value depends on the molar mass of the nucleic acids, since plasmid DNA required much higher values of $z^-_{Hep}/z^-_{RNA} > 25$ for release (42).

The particular dye labeling used in this study had been optimized before (34) and from our experience with various dye labels on RNA (20,43), we anticipated changes in both fluorescence intensity and FRET efficiency upon inclusion of labeled siRNA in polyplexes. Changes in fluorescence intensity upon complexation have been observed before (15,18,44) and were employed in complex formation studies by fluorimetry (11,15) as well as FCS (11).

However, this feature has not been evaluated in comparison of different polyplexes, and especially the fluorescence enhancement observed with nanohydrogels is remarkable. In contrast, some compounds decrease fluorescence to a degree that goes well beyond what one would expect from an inner filter effect or even Stern Volmer quenching. For poly-L-lysine brushes and block copolymers, this effect was so dominant that it rendered the exploitation of fluorescence for MST, or of FRET for integrity assessment, impossible. It also stands to reason that observation of cellular uptake by confocal laser scanning microscopy (CLSM) or quantification by FACS, both standard techniques in polyplex characterization, will suffer severe drawbacks because the fluorescence of free siRNA *versus* siRNA in polyplexes will be over- or underestimated, depending on the material used (18).

Table V Hydrodynamic Radii for Polyplexes at cc_1

Nanoparticle	Remark	R_h[a]
siRNA only		2.7 nm
Lysine brushes		60 nm
Copolymers	Measured by (28)	29 nm
Peptides	ill defined aggregates	Highly polydisperse
Lipids	Ill defined aggregates	Highly polydisperse
Nanohydrogels		22 nm
$MnO@SiO_2$ particles		18 nm

[a] hydrodynamic radius determined by FCS

In preliminary observations of cellular uptake by CLSM (20), we had hoped to exploit quenching effects for the selective visualization of siRNA released from polyplexes. However, while intact siRNA complexed by poly-L-lysine brushes was indeed barely visible, released siRNA produced a strong donor and a low FRET signal identifying it as degraded siRNA (data not shown).

To characterize the combined effects on FRET efficiency of complexation on one hand, and degradation by lytic enzymes on the other hand, we developed and applied a FRET based assessment of siRNA integrity with real-time readout. This assay responds to the siRNA fraction that is available to nucleases, and therefore free, or only partially engaged in interaction with the polyplex particles. Rather than the artificial non-equilibrium binding conditions in the EMSA, or the equilibrium conditions covered by MST, the conditions there reflect a steady state more appropriately. In this steady state, a fraction of siRNA is released from the polyplex, creating a population of intact siRNA that is available for biological activity, from which a fraction is steadily removed by nuclease activity. Given this scenario, it is apparent that neither too high nor too low binding is conductive to efficient RNAi, since the pool of free siRNA would be too low, or not available for an extended period of time, respectively.

In a second part of this work, we have employed a number of elements to link the FRET-based integrity assessment from the cuvette to settings of more physiological relevance. First we moved from challenging the polyplexes with pure RNase to using serum, which revealed surprisingly high stability of the siRNA in standard cell culture medium. As a logical consequence, we assessed integrity kinetics after uptake into the cell, still using FRET, and we also quantified the uptake. Although we have thus monitored a variety of siRNA polyplexes at various stations during their lifetime, the outcome is not a clear-cut single parameter whose optimization would directly lead to a perfect transfection reagent with high RNAi efficiency. Then again, RNAi mediated by exogenous siRNA is a complex, multi-parameter process unlikely to be governed by a single parameter. However, we have been able to determine some common characteristics of the two

polyplex types that were successful in RNAi, namely lipids and peptides. These parameters include an intermediate binding strength, as determined by purely biophysical methods EMSA, and MST on one hand. On the other hand, another striking similarity is found in the intracellular integrity measurements in Fig. 7. Both types of polyplexes show initially high integrity at 4 h, which rapidly decays until 12 h, unlike any other of the polyplex forming compounds. Admittedly, further experiments must be conducted to confirm this hypothesis.

CONCLUSION

The biological activity of siRNA polyplexes is subject to a large variety of parameters, of which only a fraction has been properly recognized and even fewer can be isolated and addressed in *in vitro* assays. Although the current state of research is still mostly based on try-and-error in cell culture assays, there is a noticeably tendency to isolate and optimize single parameters of siRNA polyplexes. Fluorescent labels are an important strategy in this endeavor, and our current work not only makes use of a sophisticated double-label FRET system, but also reveals variegated influences of different materials assessed in polyplex formation. This has important impact in experiments trying to quantitate siRNA uptake by fluorescence CLSM and FACS based methods alike, because the fraction of free or polyplex bound siRNA will be misestimated. Hence, changes in fluorescence of labeled siRNA upon polyplex formation need to be more systematically investigated for better coherence of observation results of polyplex formation and uptake in the field.

Our approach to use a panel with structurally and chemically highly diverse nanoscale polyplexes has enabled us to assess a comparatively large range of binding strength and other characteristics in a comparative fashion. In doing so, we have revealed certain drawbacks in conventional EMSA experiments, which are most likely due to the non-equilibrium conditions intrinsic to electrophoresis. As alternatives, we introduce two new methods for the efficient and informative characterization of siRNA polyplexes.

MST is a fast and reproducible equilibrium method with a range of buffer and temperature conditions available. Our FRET based degradation assay simulates a steady state during which there is a continuous release of siRNA from polyplexes, of which a part is subject to nuclease degradation while a relatively stable fraction is free and available for the RNAi machinery. Both methods can reflect and assess the entire range of binding strengths available in the panel of polyplexes. Most interestingly, the two compounds that were found active in RNAi of a reporter gene, display intermediate behavior among the panel compounds, as well as particular kinetics of intracellular degradation. While the current dataset, although vast, cannot unambiguously confirm these characteristics as the crucially important ones, they represent a promising starting point for future research.

ACKNOWLEDGMENTS AND DISCLOSURES

This work was supported by the DFG in the frame of the collaborative research center, featuring project grant A7 to M.H., A6 to M.S., B2 to K.K., A3 to W.T., A4 to R.Z. The cylindrical brush sample was synthesized by Dr. Mike Sahl, Institute for Physical Chemistry, University Mainz, which is gratefully acknowledged. Flow cytometry was kindly supported by the Cytometry Core Facility of the Institute of Molecular Biology (IMB), Mainz.

REFERENCES

1. Diken M, Kreiter S, Selmi A, Britten CM, Huber C, Türeci Ö, *et al.* Selective uptake of naked vaccine RNA by dendritic cells is driven by macropinocytosis and abrogated upon DC maturation. Gene Ther. 2011;18(7):702–8.
2. Gooding M, Browne LP, Quinteiro FM, Selwood DL. siRNA delivery: from lipids to cell-penetrating peptides and their mimics. Chem Biol Drug Des. 2012;80(6):787–809.
3. Gao Y, Liu X-L, Li X-R. Research progress on siRNA delivery with nonviral carriers. Int J Nanomedicine. 2011;6:1017–25.
4. Vader P, van der Aa LJ, Engbersen JFJ, Storm G, Schiffelers RM. Physicochemical and biological evaluation of siRNA polyplexes based on PEGylated Poly(amido amine)s. Pharm Res. 2012;29(2):352–61.
5. Ruponen M, Ylä-Herttuala S, Urtti A. Interactions of polymeric and liposomal gene delivery systems with extracellular glycosaminoglycans: physicochemical and transfection studies. Biochim Biophys Acta. 1999;1415(2):331–41.
6. Nguyen J, Reul R, Roesler S, Dayyoub E, Schmehl T, Gessler T, *et al.* Amine-modified poly(vinyl alcohol)s as non-viral vectors for siRNA delivery: effects of the degree of amine substitution on physicochemical properties and knockdown efficiency. Pharm Res. 2010;27(12):2670–82.
7. Sato A, Choi SW, Hirai M, Yamayoshi A, Moriyama R, Yamano T, *et al.* Polymer brush-stabilized polyplex for a siRNA carrier with long circulatory half-life. J Control Release Off J Control Release Soc. 2007;122(3):209–16.
8. Kim M, Kim HR, Chae SY, Larson RG, Lee H, Park JC. Effect of arginine-rich peptide length on the structure and binding strength of siRNA-peptide complexes. J Phys Chem B. 2013;117(23):6917–26.
9. Crombez L, Aldrian-Herrada G, Konate K, Nguyen QN, McMaster GK, Brasseur R, *et al.* A new potent secondary amphipathic cell-penetrating peptide for siRNA delivery into mammalian cells. Mol Ther. 2009;17(1):95–103.
10. Wagner M, Rinkenauer AC, Schallon A, Schubert US. Opposites attract: influence of the molar mass of branched poly(ethylene imine) on biophysical characteristics of siRNA-based polyplexese. RSC Adv. 2013;3(31):12774.
11. Van Rompaey E, Engelborghs Y, Sanders N, De Smedt SC, Demeester J. Interactions between oligonucleotides and cationic polymers investigated by fluorescence correlation spectroscopy. Pharm Res. 2001;18(7):928–36.

12. Pereira P, Jorge AF, Martins R, Pais A, Sousa F, Figueiras A. Characterization of polyplexes involving small RNA. J Colloid Interface Sci. 2012;387(1):84–94.
13. Buyens K, Meyer M, Wagner E, Demeester J, De Smedt SC, Sanders NN. Monitoring the disassembly of siRNA polyplexes in serum is crucial for predicting their biological efficacy. J Control Release. 2010;141(1):38–41.
14. Varkouhi AK, Mountrichas G, Schiffelers RM, Lammers T, Storm G, Pispas S, *et al.* Polyplexes based on cationic polymers with strong nucleic acid binding properties. Eur J Pharm Sci. 2012;45(4):459–66.
15. Zheng M, Pavan GM, Neeb M, Schaper AK, Danani A, Klebe G, *et al.* Targeting the blind spot of polycationic nanocarrier-based siRNA delivery. ACS Nano. 2012;6(11):9447–54.
16. Gary DJ, Min J, Kim Y, Park K, Won Y-Y. The effect of N/P ratio on the in vitro and in vivo interaction properties of PEGylated poly[2-(dimethylamino)ethyl methacrylate]-based siRNA complexes. Macromol Biosci. 2013;13(8):1059–71.
17. Ouyang D, Zhang H, Parekh HS, Smith SC. Structure and dynamics of multiple cationic vectors-siRNA complexation by all-atomic molecular dynamics simulations. J Phys Chem B. 2010;114(28):9231–7.
18. Vader P, van der Aa LJ, Engbersen JFJ, Storm G, Schiffelers RM. A method for quantifying cellular uptake of fluorescently labeled siRNA. J Control Release Off J Control Release Soc. 2010;148(1):106–9.
19. Jensen LB, Griger J, Naeye B, Varkouhi AK, Raemdonck K, Schiffelers R, *et al.* Comparison of polymeric siRNA nanocarriers in a murine LPS-activated macrophage cell line: gene silencing, toxicity and off-target gene expression. Pharm Res. 2012;29(3):669–82.
20. Järve A, Müller J, Kim I-H, Rohr K, MacLean C, Fricker G, *et al.* Surveillance of siRNA integrity by FRET imaging. Nucleic Acids Res. 2007;35(18):e124.
21. Vuorimaa E, Urtti A, Seppänen R, Lemmetyinen H, Yliperttula M. Time-resolved fluorescence spectroscopy reveals functional differences of cationic polymer-DNA complexes. J Am Chem Soc. 2008;130(35):11695–700.
22. Buyens K, Lucas B, Raemdonck K, Braeckmans K, Vercammen J, Hendrix J, *et al.* A fast and sensitive method for measuring the integrity of siRNA-carrier complexes in full human serum. J Control Release Off J Control Release Soc. 2008;126(1):67–76.
23. Lucas B, Remaut K, Sanders NN, Braeckmans K, De Smedt SC, Demeester J. Studying the intracellular dissociation of polymer-oligonucleotide complexes by dual color fluorescence fluctuation spectroscopy and confocal imaging. Biochemistry. 2005;44(29):9905–12.
24. Wang M, Adikane HV, Duhamel J, Chen P. Protection of oligodeoxynucleotides against nuclease degradation through association with self-assembling peptides. Biomaterials. 2008;29(8):1099–108.
25. Uchiyama H, Hirano K, Kashiwasake-Jibu M, Taira K. Detection of undegraded oligonucleotides in vivo by fluorescence resonance energy transfer. Nuclease activities in living sea urchin eggs. J Biol Chem. 1996;271(1):380–4.
26. Remaut K, Lucas B, Braeckmans K, Sanders NN, Demeester J, De Smedt SC. Protection of oligonucleotides against nucleases by pegylated and non-pegylated liposomes as studied by fluorescence correlation spectroscopy. J Control Release. 2005;110(1):212–26.
27. Sahl M, Muth S, Branscheid R, Fischer K, Schmidt M. Helix−coil transition in cylindrical brush polymers with poly-L-lysine side chains. Macromolecules. 2012;45:5167–75.
28. Tabujew I, Freidel C, Krieg B, Helm M, Koynov K, Müllen K, *et al.* The guanidinium group as a key part of water-soluble polymer carriers for siRNA complexation and protection against degradation. Macromol Rapid Commun. 2014;35(13):1191–7.
29. Lam JKW, Liang W, Lan Y, Chaudhuri P, Chow MYT, Witt K, *et al.* Effective endogenous gene silencing mediated by pH responsive peptides proceeds via multiple pathways. J Control Release Off J Control Release Soc. 2012;158(2):293–303.
30. Nuhn L, Hirsch M, Krieg B, Koynov K, Fischer K, Schmidt M, *et al.* Cationic nanohydrogel particles as potential siRNA carriers for cellular delivery. ACS Nano. 2012;6(3):2198–214.
31. Nuhn L, Gietzen S, Mohr K, Fischer K, Toh K, Miyata K, *et al.* Aggregation behavior of cationic nanohydrogel particles in human blood serum. Biomacromolecules. 2014;15(4):1526–33.
32. Schladt TD, Koll K, Prüfer S, Bauer H, Natalio F, Dumele O, *et al.* Multifunctional superparamagnetic MnO@SiO2 core/shell nanoparticles and their application for optical and magnetic resonance imaging. J Mater Chem. 2012;22(18):9253.
33. Kitsera N, Khobta A, Epe B. Destabilized green fluorescent protein detects rapid removal of transcription blocks after genotoxic exposure. Biotechniques. 2007;43(2):222–7.
34. Hirsch M, Strand D, Helm M. Dye selection for live cell imaging of intact siRNA. Biol Chem. 2012;393(1–2):23–35.
35. Seidu-Larry S, Krieg B, Hirsch M, Helm M, Domingo O. A modified guanosine phosphoramidite for click functionalization of RNA on the sugar edge. Chem Commun (Camb). 2012;48(89):11014–6.
36. Hirsch M, Ziroli V, Helm M, Massing U. Preparation of small amounts of sterile siRNA-liposomes with high entrapping efficiency by dual asymmetric centrifugation (DAC). J Control Release Off J Control Release Soc. 2009;135(1):80–8.
37. Adenier A, Aaron JJ. A spectroscopic study of the fluorescence quenching interactions between biomedically important salts and the fluorescent probe merocyanine 540. Spectrochim Acta A Mol Biomol Spectrosc. 2002;58(3):543–51.
38. Trubetskoy VS, Slattum PM, Hagstrom JE, Wolff J, Budker VG. Quantitative assessment of DNA condensation. Anal Biochem. 1999;267(2):309–13.
39. Kim I-H, Järve A, Hirsch M, Fischer R, Trendelenburg MF, Massing U, *et al.* FRET imaging of cells transfected with siRNA/liposome complexes. In: Weissig V, editor. Liposomes methods and protocols. Berlin: Springer; 2010. p. 439–55.
40. Troiber C, Kasper JC, Milani S, Scheible M, Martin I, Schaubhut F, *et al.* Comparison of four different particle sizing methods for siRNA polyplex characterization. Eur J Pharm Biopharm. 2013;84(2):255–64.
41. Jerabek-Willemsen M, Wienken CJ, Braun D, Baaske P, Duhr S. Molecular interaction studies using microscale thermophoresis. Assay Drug Dev Technol. 2011;9(4):342–53.
42. Hedrich J, Wu Y, Kuan S, Kühn F, Pietrowski E, Sahl M, *et al.* Polymer complexes in biological applications. In: Basché T, Müllen K, Schmidt M, editors. From single molecules to nanoscopically structured materials. Berlin: Springer; 2014. p. 211–35.
43. Kobitski AY, Hengesbach M, Seidu-Larry S, Dammertz K, Chow CS, van Aerschot A, *et al.* Single-molecule FRET reveals a cooperative effect of two methyl group modifications in the folding of human mitochondrial tRNA(Lys). Chem Biol. 2011;18(7):928–36.
44. Jafari M, Xu W, Naahidi S, Chen B, Chen P. A new amphipathic, amino-acid-pairing (AAP) peptide as siRNA delivery carrier: physicochemical characterization and in vitro uptake. J Phys Chem B. 2012;116(44):13183–91.